Coupling between surface plasmons and nonresonant transmission in subwavelength holes at terahertz frequencies

Jiaguang Han, Abul K. Azad, Mufei Gong, Xinchao Lu, and Weili Zhang[a)]
School of Electrical and Computer Engineering, Oklahoma State University, Stillwater, Oklahoma 74078

(Received 4 May 2007; accepted 23 July 2007; published online 17 August 2007)

Transmission spectra of terahertz pulses through periodic array of subwavelength holes exhibit a characteristic evolution with various hole widths. The peak absolute transmittance approaches a maximum value at a critical hole width, while linewidth broadening and blueshift of peak frequency are observed with increasing hole width. Such characteristic evolution is attributed to the coupling between discrete resonant excitation of surface plasmons and continuum nonresonant transmission through the holes; this agrees well with the numerical analysis based on the Fano model and the measured angle-resolved transmission band structures. © *2007 American Institute of Physics*. [DOI: 10.1063/1.2771093]

Extraordinary transmission of electromagnetic waves through periodic array of subwavelength holes has attracted enormous interest in both the understanding of its origin and the fascinating applications in a variety of fields.[1–5] In the terahertz regime, highly conductive properties of metals have enabled unique transmission characteristics of periodic subwavelength structures.[6–14] Extraordinary terahertz transmission was demonstrated in arrays of subwavelength holes made even from Pb, a generally poor metal.[15] Surface plasmons (SPs) excited at the surface of subwavelength hole arrays were demonstrated to play a dominant role in the extraordinary transmission.[1,16,17] Recent studies have also revealed that besides SPs, localized effects also make contributions to the extraordinary transmission of light in periodic subwavelength holes.[4,18,19]

In this letter, to better understand such transmission enhancement in the terahertz regime, we study a series of subwavelength hole arrays with various hole widths. The measured hole width-dependent transmission spectra present a characteristic evolution, including well-regulated change in transmittance, linewidth broadening, and blueshift of peak frequencies.[4] Based on numerical analysis by the Fano model and the momentum-dependent transmission measurements, we find that the transmission properties of periodic subwavelength holes in the terahertz regime are associated with both resonant excitation of SPs and nonresonant transmission (or non-SP transmission); the latter exhibits angle-independent peak frequencies and could be resulted from localized effects and direct transmission.[4,18–23] The localized effects, as either localized modes or localized waveguide resonances,[4,18,19] also contribute substantially to the enhanced transmission of terahertz pulses. The direct transmission, on the other hand, due to scattering and low filling fraction of metal, is the origin that causes the reduction in transmission efficiency of the holes.

Hexagonal arrays of rectangular subwavelength holes are a lithographically fabricated 180-nm-thick Al film onto a 0.64-mm-thick silicon wafer (p-type resistivity 20 Ω cm, inset of Fig. 1). Each sample, with dimensions of 15 $\times$ 15 mm^2, has holes of a fixed length 120 μm and various widths from 40 to 140 μm with a 20 μm interval, and a constant lattice period of 160 μm. A blank silicon slab identical to the array substrate is used to obtain the reference terahertz pulses. The arrays are characterized by a broadband terahertz time-domain spectroscopy (TDS) system configured with an 8-F confocal geometry.[15,24] The sample is placed midway between the photoconductive transmitter and receiver in the far field at a 3.5 mm frequency-independent beam waist. The P-polarized terahertz electric field is perpendicular to the fixed axis of the holes. The absolute transmittance is defined as $T(\omega)=|t(\omega)|^2=|E_{\text{out}}(\omega)/E_{\text{in}}(\omega)|^2$, where $|t(\omega)|$ is the amplitude transmission and $E_{\text{out}}(\omega)$ and $E_{\text{in}}(\omega)$ are the amplitudes of terahertz pulses through the sample and reference, respectively.

Figure 1(a) illustrates the measured transmitted terahertz pulses through the reference and an array with hole dimen-

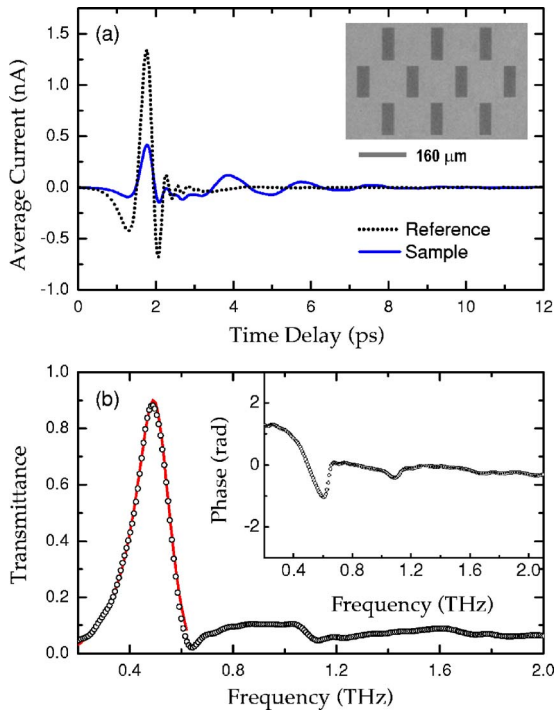

FIG. 1. (Color online) (a) Measured transmitted terahertz pulses through the reference and the 120$\times$40 μm^2 hole array. Inset: a scanning electron microscopy image of the array. (b) Measured (open circles) and the Fano fit (solid curve) of transmittance. The fitting parameters are $q_v=26.5\pm0.2$, $\omega_v/2\pi=0.49\pm0.05$ THz, $\Gamma_v/2\pi=0.16\pm0.01$ THz, and $T_b=(1.28\pm0.1)\times10^{-3}$ for the $[\pm1,0]$ mode. Inset: corresponding data of phase change.

[a)]Electronic mail: wwzhang@okstate.edu

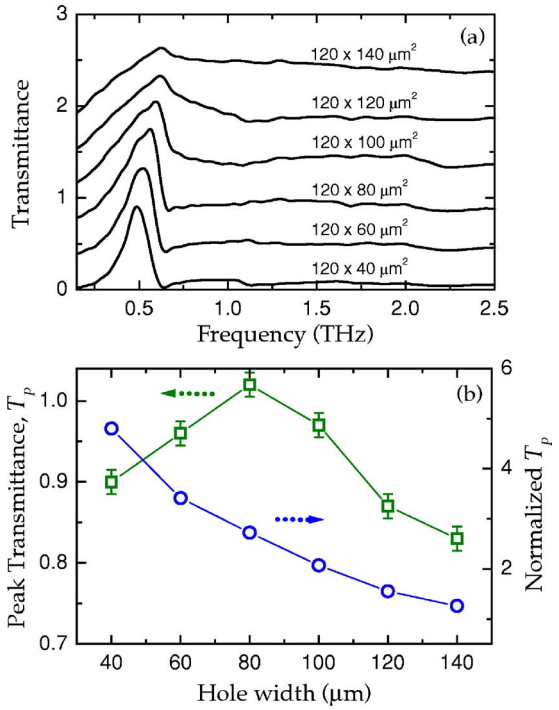

FIG. 2. (Color online) (a) Measured absolute transmittance of the hole arrays with fixed hole length of 120 μm and various hole widths. For clarity, the curves are vertically displaced by 0.36. (b) Absolute (squares) and normalized (circles) peak transmittance as a function of hole width. The solid lines are guides for the eye.

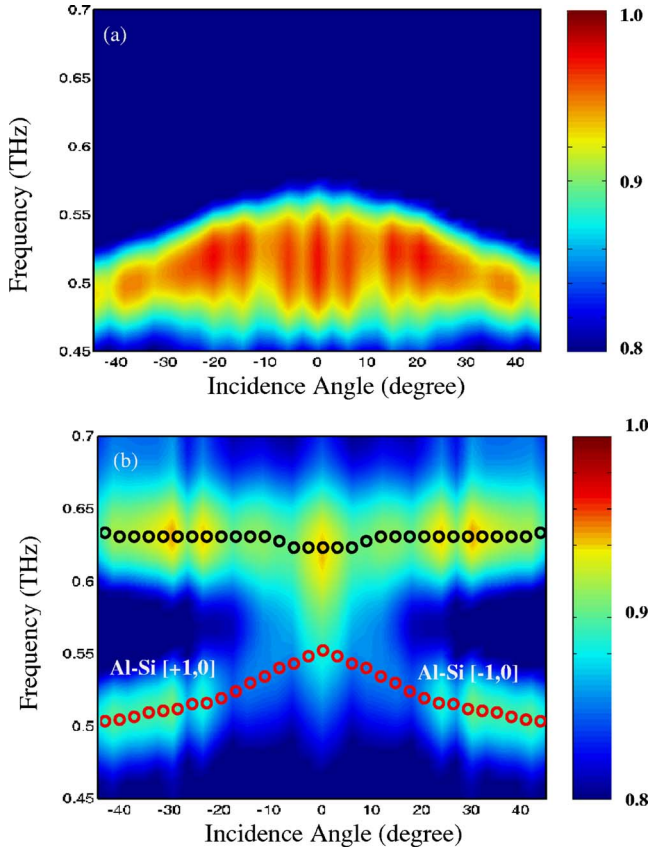

FIG. 3. (Color online) Angle-dependent amplitude transmission for arrays with hole dimensions of (a) 120×60 μm^2 and (b) 120×120 μm^2. The open circles represent the peak frequencies of the Al–Si SP $[\pm1,0]$ modes and nonresonant transmission.

sions of 120×40 μm^2. The extracted frequency-dependent absolute transmittance is illustrated as open circles in Fig. 1(b), while the inset shows the corresponding phase change $\phi(\omega)=\arg[t(\omega)]$. In such hole arrays, SPs can be resonantly excited at the Al–Si interface by conserving the momentum match: $\mathbf{k}_{SP}=\mathbf{k}_{\parallel}+\mathbf{G}$, where $\mathbf{k}_{SP}$ is the wave vector of SPs, $\mathbf{k}_{\parallel}$ is the in-plane wave vector with $k_{\parallel}=(\omega/c)\sin\theta$, $\mathbf{G}$ is the reciprocal lattice vectors, and θ is the incidence angle.[1] At normal incidence, the in-plane wave vector becomes zero. The calculated fundamental SP $[\pm1,0]$ resonance of hexagonal arrays at the Al–Si interface is around 0.63 THz, which is higher than the measured transmission peak at 0.49 THz; the latter is a result of both resonant and nonresonant contributions.[1,6,7,25,26]

The measured transmittance is analyzed by the Fano model that involves two types of scattering processes: one refers to the continuum direct scattering state and the other is the discrete resonant state.[23,25,27–30] For an isolated resonance, the Fano model can be written as $T_{\mathrm{Fano}}(\omega)=|t(\omega)|^2=T_a+T_b(\varepsilon_v+q_v)^2/(1+\varepsilon_v^2)$, where $\varepsilon_v=(\omega-\omega_v)/(\Gamma_v/2)$, T_a is a slowly varying transmittance, and $|T_b|$ is the contribution of a zero-order continuum state that couples with the discrete resonant state. The resonant state is characterized by the resonance frequency ω_v, the linewidth Γ_v, and the Breit-Wigner-Fano coupling coefficient q_v.[23,25,27–30] Considering that such transmission behavior resulted from two contributions—the resonant excitation of SPs as the discrete resonant state and the direct continuum state, namely, the nonresonant terahertz transmission—the Fano model provides a consistent fit (solid curve) to the measured transmittance shown in Fig. 1(b), with a peak transmission at $\omega_v/2\pi=0.49$ THz and a linewidth $\Gamma_v/2\pi=0.16$ THz.

To understand clearly the coupling between SPs and nonresonant transmission, we have characterized arrays with various hole widths from 40 to 140 μm. The measured transmittance of these arrays shown in Fig. 2(a) reveals a characteristic evolution with respect to hole widths. The peak absolute transmittance T_P (squares) is enhanced with increasing hole width of up to 80 μm; however, the further increase in hole width beyond 80 μm gives rise to a monotonic decay in T_P, as depicted in Fig. 2(b). This suggests that there exists an optimal hole width, at which T_P approaches a maximum value. Meanwhile, the resonance frequency and the corresponding linewidth exhibit monotonic changes. As the hole width increases from 40 to 140 μm, the peak transmission is shifted from 0.49 to 0.63 THz, while the corresponding linewidth is broadened from 0.16 to $\sim$0.66 THz.

Taking the contribution of in-plane wave vector $k_{\parallel}=(\omega/c)\sin\theta$ into account, the resonance frequency of SPs exhibits dependence on incidence angle θ, whereas the nonresonant transmission is angle independent.[20] Figure 3(a) illustrates the full band structure of an array with hole dimensions of 120×60 μm^2, where the resolved resonance frequencies of the Al–Si $[\pm1,0]$ mode shows dependence on incidence angles. This array of narrow hole width corresponds to 2:1 relatively high aspect ratio and 72% high filling fraction of metal; this enables SPs to be well pronounced at the Al–Si interface and hence SPs along with localized effects play dominant roles in the enhanced transmission.[18,19] The increase in hole width, however, will result in lower aspect ratio, lower filling fraction of metal,[4] and lower cutoff frequencies of the holes as well. This consequently enhances

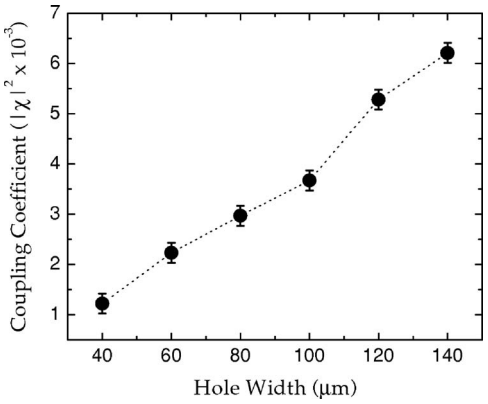

FIG. 4. Calculated coupling coefficient of the Al–Si SP [±1,0] modes with non-resonant transmission for different hole widths at normal incidence. The dotted line is a guide for the eye.

direct transmission which is a part of nonresonant transmission, and the coupling of nonresonant transmission toward SPs also increases.

Figure 3(b) shows the angle-dependent measurements on the array with hole dimensions of 120×120 μm^2, with a relatively low aspect ratio of 1:1 and a low filling fraction of metal of 44%. The maximum transmission located at 0.63 THz exhibits an angle-independent behavior, which is mainly ascribed to the contribution of increased direct transmission due to large hole width. The angle-dependent low-frequency peak near 0.55 THz is originated from the Al–Si SP [±1,0] mode. An energy gap greater than 0.36 meV is observed between the two transmission peaks at incident angles above 9°.

As described in the Fano model, the total transmission is determined by the resonant and nonresonant states and the coupling between them. The all-out transmission probability can be obtained by solving the Hamiltonian, $\hat{H}=\hat{H}_{SP}+\hat{H}_{NRT}+\hat{H}_{coupling}$. Hence, the coupling can be evaluated by diagonalizing the Hamiltonian matrix,[13,25,28]

$$H=\hbar\begin{pmatrix}\omega_{SP} & \chi\\ \chi^{*} & \omega_{NRT}\end{pmatrix}, \tag{1}$$

where ω_{SP} is the resonance frequency of the SP mode given based on the momentum relationship, ω_{NRT} is the frequency of nonresonant transmission, and χ is the coupling coefficient between SPs and nonresonant transmission. Based on the measured angle-dependent results on each array of different hole widths, we solve the coupling $|\chi|^2$ at each angle of incidence.

Figure 4 shows the calculated coupling strength between the SP mode and nonresonant transmission for arrays with different hole widths at normal incidence. With increasing hole width the coupling strength shows monotonic change; it is enhanced from $|\chi|^2=1.22\times10^{-3}$ at 40 μm to $|\chi|^2=6.21\times10^{-3}$ at 140 μm. Thus, the increase in hole width, which corresponds to reduced aspect ratio of holes and lower filling fraction of metal, not only leads to increased direct transmission through the holes but also enhances the coupling between SPs and nonresonant transmission. This in turn gives rise to an increased damping of SPs and thus the line width broadens and shifts to higher frequencies toward the peak of nonresonant transmission.[4,20–23,28] Another evidence of the effect of direct transmission due to increased hole width is that, when the peak absolute transmittance T_P is normalized by the area of the holes, as shown by the circles in Fig. 2(b), it exhibits monotonic decrease with increasing hole width.

The maximum absolute peak transmittance T_P achieved at hole width 80 μm (aspect ratio of 3:2 and filling fraction of metal of 62.5%) indicates that the negative effect of direct transmission becomes critical and challenges the dominant role of SPs and localized effects when the hole width is further increased. The contributions of localized effects and direct transmission to the effect of nonresonant transmission could vary with various hole widths (or aspect ratio) and filling fraction of metal. For arrays with filling fraction of metal less than 80%, direct transmission contributes substantially to nonresonant transmission and causes the normalized transition efficiency to decline monotonically.

The authors acknowledge the efforts of S. Ray, R. Sleezer, and D. Ganta. One of the authors (A.K.A.) is now with the Los Alamos National Laboratory. This study is supported by the National Science Foundation.

[1] T. W. Ebbesen, H. J. Lezec, H. F. Ghaemi, T. Thio, and P. A. Wolff, Nature (London) **391**, 667 (1998).
[2] W. L. Barnes, A. Dereux, and T. W. Ebbesen, Nature (London) **424**, 824 (2003).
[3] R. Gordon, M. Hughes, B. Leathem, K. L. Kavanagh, and A. G. Brolo, Nano Lett. **5**, 1243 (2005).
[4] K. Molen, K. Koerkamp, S. Enoch, F. Segerink, N. Kulst, and L. Kuipers, Phys. Rev. B **72**, 045421 (2005).
[5] L. Martín-Moreno, F. J. García-Vidal, H. J. Lezec, A. Degiron, and T. W. Ebbesen, Phys. Rev. Lett. **90**, 167401 (2003).
[6] D. Qu, D. Grischkowsky, and W. Zhang, Opt. Lett. **29**, 896 (2004).
[7] G. Torosyan, C. Rau, B. Pradarutti, and R. Beigang, Appl. Phys. Lett. **85**, 3372 (2004).
[8] J. O'Hara, R. D. Averitt, and A. J. Taylor, Opt. Express **12**, 6397 (2004).
[9] J. Saxler, J. G. Rivas, C. Janke, H. P. M. Pellemans, P. H. Bolver, and H. Kurz, Phys. Rev. B **69**, 155427 (2004).
[10] H. Cao and A. Nahata, Opt. Express **12**, 1004 (2004).
[11] F. Miyamaru and M. Hangyo, Appl. Phys. Lett. **84**, 2742 (2004).
[12] J. W. Lee, M. A. Seo, D. J. Park, D. S. Kim, S. C. Jeoung, C. Lienau, Q. H. Park, and P. C. M. Planken, Opt. Express **14**, 1253 (2006).
[13] J. B. Masson and G. Gallot, Phys. Rev. B **73**, 121401 (2006).
[14] Q. Xing, S. Li, Z. Tian, D. Liang, N. Zhang, L. Lang, L. Chai, and Q. Wang, Appl. Phys. Lett. **89**, 041107 (2006).
[15] A. K. Azad, M. He, Y. Zhao, and W. Zhang, Opt. Lett. **31**, 2637 (2006); A. K. Azad and W. Zhang, *ibid.* **30**, 2945 (2005).
[16] H. Raether, *Surface Plasmons on Smooth and Rough Surfaces and on Gratings* (Springer, Berlin, 1988), Chap. 2, p. 4.
[17] E. Ozbay, Science **311**, 189 (2006).
[18] Z. Ruan and M. Qiu, Phys. Rev. Lett. **96**, 233901 (2006).
[19] A. Degiron and T. W. Ebbesen, J. Opt. A, Pure Appl. Opt. **7**, S90 (2005).
[20] D. S. Kim, S. C. Hohng, V. Mayarchuk, Y. C. Yoon, Y. H. Ahn, K. J. Yee, J. W. Park, J. Kim, Q. H. Park, and C. Lienau, Phys. Rev. Lett. **91**, 143901 (2003).
[21] T. Matsui, A. Agrawal, A. Nahata, and Z. V. Vardeny, Nature (London) **446**, 517 (2007).
[22] F. J. García de Abajo, J. Sáenz, I. Campillo, and J. Dolado, Opt. Express **14**, 7 (2006).
[23] W. Zhang, A. K. Azad, J. Han, J. Xu, J. Chen, and X.-C. Zhang, Phys. Rev. Lett. **98**, 183901 (2007).
[24] D. Grischkowsky, S. Keiding, M. Van Exter, and Ch. Fattinger, J. Opt. Soc. Am. B **7**, 2006 (1990).
[25] C. Genet, M. P. Van Exter, and J. P. Woerdman, Opt. Commun. **225**, 331 (2003).
[26] H. J. Lezec and T. Thio, Opt. Express **12**, 3629 (2004).
[27] U. Fano, Phys. Rev. **124**, 1866 (1961).
[28] W. Fan, S. Zhang, B. Minhas, K. J. Malloy, and S. R. J. Brueck, Phys. Rev. Lett. **94**, 033902 (2005).
[29] M. Sarrazin, J. Vigneron, and J. Vigoureux, Phys. Rev. B **67**, 085415 (2003).
[30] S. H. Chang, S. K. Gray, and G. C. Schatz, Opt. Express **13**, 3150 (2005).